Supporting Information (SI)

Construction of S-scheme heterojunctions of Ti doped Ce-MOF and BiOCl for efficient photocatalytic selective oxidation of amines

Danxia Zhao,*[a,b] Pengyu Wu[c], Huayue Zhu[a,b], Ru jiang[a,b], Jingwei Chen[a], Chuhan Qiu[a], Shengtao Jiang[a] and Guoping Lu[d]*

*[a] Institute of Environmental Engineering Technology, Taizhou University, Taizhou 318000, Zhejiang, P. R. China **.

*b Zhejiang Provincial Key Laboratory of Plant Evolutionary Ecology and Conservation, Taizhou University, Taizhou, Zhejiang 318000, P. R. China **. E-mail: danxia@tzc.edu.cn; danxia@126.com.*

c Key Laboratory for Advanced Technology in Environmental Protection of Jiangsu Province, Yancheng Institute of Technology, Jiangsu 224051, P. R. China.

d Nanjing University of Science and Technology, School of Chemical Engineering, 200 Xiaoling Wei, Nanjing, Jiangsu 210094, P. R. China. E-mail: glu@njust.edu.cn.

Experimental

Preparation of UiO-66(Ce/Ti)

The bimetallic UiO-66(Ce/Ti) was prepared by incorporating Ti into UiO-66(Ce) via facile cation exchange. The $TiCp_2Cl_2$ (97.5 mg) and the UiO-66(Ce) crystals (130 mg) were mixed in 25 mL DMF with vigorous stirring. The obtained homogeneous liquid was transferred to a 50 mL round-bottom flask, and kept at 100 °C for 3 h and then cooled down to the room temperature. The product UiO-66(Ce/Ti) was collected by centrifugation and washed three times with DMF and ethanol respectively. The resultant UiO-66(Ce/Ti) crystals were collected and dried under vacuum at 80 °C before use.

Preparation of BiOCl/UiO-66(Ce/Ti) (BCT)

In a typical procedure, 200 mg UiO-66(Ce/Ti) and 5 mmol $KMnO_4$ were each dissolved in 20 ml of de-ionized water, and the former was ultrasonically dispersed for 30 min to form a homogeneous suspension (denoted as solution A). 5 mmol $BiCl_3$ was dissolved in 30 ml ethylene glycol to form a homogeneous solution B. Subsequently, the prepared A and B solution was added dropwise to the $KMnO_4$ solution under continuous stirring. After 2 h, the obtained mixture was moved to a 100 mL Teflon-lined stainless steel autoclave and heated at 160 °C for 6 h and a brown powder product was obtained. Finally, the resultant BiOCl/UiO-66(Ce/Ti) compound (named as BCT) was centrifuged and washed with de-ionized water and ethanol several times before being dried at 70 °C for 12 h. For comparison, the pure BiOCl was prepared according to the same procedure except for the precursor without UiO-66(Ce/Ti) crystals.

Experimental Methods

Characterization of photocatalysts

X-ray diffractometry (XRD) using a Shimadzu XRD-6000 diffractometer with Cu Kα irradiation. Fourier transform infrared (FTIR) spectroscopy was performed at 8 cm^{-1} resolution in the range of 400-4000 cm^{-1} on a Nicolet iS10 FTIR spectrometer. Scanning electron microscopy (SEM) images was performed using a Hitachi S-4800. TEM images were taken using a PHILIPS Tecnai 12 microscope operating at 120 kv. Energy Dispersive X-ray Spectroscopic analysis (EDS) was performed with a JEM-

2010(HR) transmission electron microscope at an acceleration voltage of 200kV. High Resolution Transmission electron microscopy (HRTEM) was performed on Philips-FEI Tecnai G2 F20 operating at 300kv. In addition, the in situ XPS measurements were carried out on an ESCALAB 250Xi spectrometer (Thermo Scientific, USA) under light irradiation (365-800nm) or dark conditions. All samples were analyzed under a pressure of less than 1.0×10^{-9} Pa. Spectra were acquired through the avantage software (Version 5.979) with a step of 0.05 e V. The UV-Vis diffuse reflectance spectra of the catalysts were recorded on a UV-Vis spectrometer (Lambda 750) within the range of 200 - 1100 nm. Photoluminescence spectra (PL) of the catalysts were carried out on a spectrophotometer (LabRAM HR Evolution).

Electrochemical measurements

Electrochemical and photoelectrochemical measurements were carried out on an electrochemical workstation (CHI 660E, Shanghai) with a standard three-electrode system. The powder coated on indium-tin-oxide (ITO) glass substrate was applied as the working electrode. 10 mg powder was suspended into 1 mL absolute ethanol and then the slurry was dropwise added on a ITO substrate (15 mm × 30 mm). The working electrode was exposed to air for 10 h to remove the ethanol. Platinum wire and Ag/AgCl electrode were used as the counter electrode and reference electrode, respectively. The electrolyte was 0.1 M Na_2SO_4 solution and illumination source was a 300 W Xe lamp providing simulated solar light.

EPR measurements

EPR spectra using TEMP as a trapping agent were recorded using a Wilmad WG-810-A quartz flat cell in a mixture of O_2^-substrated H_2O/MeOH (1:4 v/v) of BCT (4 mg mL^{-1}) and TEMP (1.2 M). ESR spectra utilizing DMPO as a trapping agent were recorded using a Wilmad WG-810-A quartz flat cell in a mixture in O_2^-substrated H_2O/MeOH (1:4 v/v) of BCT (4 mg mL-1) and DMPO (1.8 M). ESR analysis was carried out at microwave frequency of 9.21 GHz at 298 K in the dark or under visible light ($\lambda > 420$ nm).

Computational methodologies and models

First-principle density-functional-theory (DFT) calculations have been performed through the Vienna ab initio simulation package (VASP) code.[1, 2] The electron-ion interactions were treated via the projector augmented wave (PAW)[3] method. The electronic exchange and correlation effects were approximated with

the Perdew-Burke-Ernzerhof (PBE)-type of generalized gradient approximation (GGA).[4] The cut-off energy for plane wave is set to 480 eV. The energy criterion is set to 10^{-4} eV in the iterative solution of the Kohn-Sham equation. To avoid interlaminar interactions, a vacuum spacing of 20 Å is applied perpendicular to the slab. The Brillouin zone integration is performed using a $2\times2\times1$ k-mesh. All the structures are relaxed until the residual forces on the atoms have declined to less than 0.05 eV/Å. To improve the accuracy of the electronic properties, the Hubbard U correction[5] for the on-site Coulomb (4 eV for Ti and 5 eV for Ce) is applied. Using pre-optimized bulk lattice parameters and atomic coordinates, the interfacial configuration was constructed by coupling the (001) surface of the UiO-66 with the (001) surface of BiOCl. Data analysis and visualization are carried out with the help of VASPKIT[6] code and VESTA[7]. The adhesive energy E_{ads} is expressed as

$$E_{ads,\,BiOCl/MOF-C7H9N} = E_{BiOCl/MOF-C7H9N} - E_{BiOCl/MOF} - E_{C7H9N} \quad (1)$$

$$E_{ads,\,BiOCl-C7H9N} = E_{BiOCl-C7H9N} - E_{BiOCl} - E_{C7H9N} \quad (2)$$

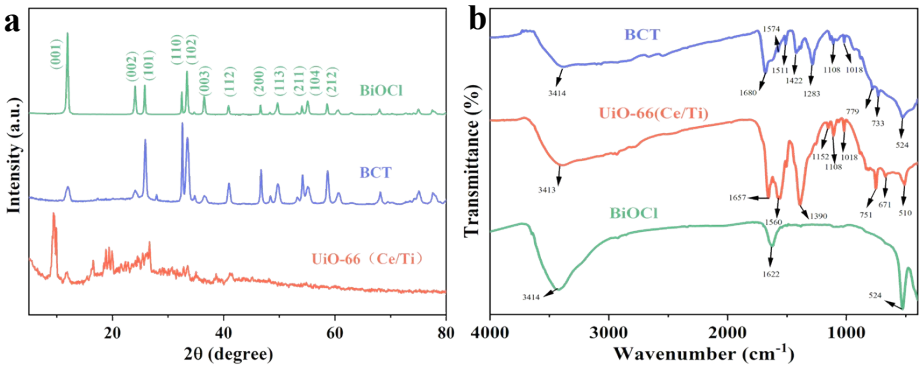

Fig. S1 a) XRD patterns, and b) Fourier transform infrared spectra of BiOCl, UiO-66(Ce/Ti) and BCT.

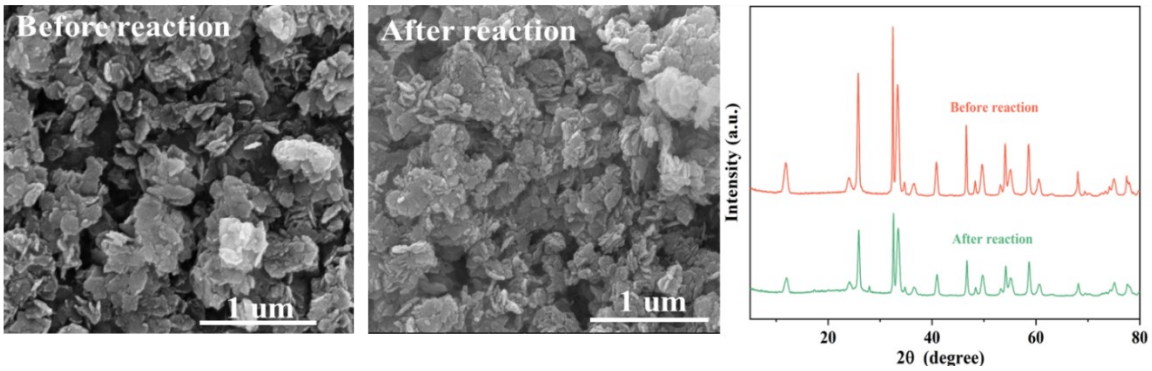

Fig. S2 SEM images and XRD before and after the photocatalytic reaction.

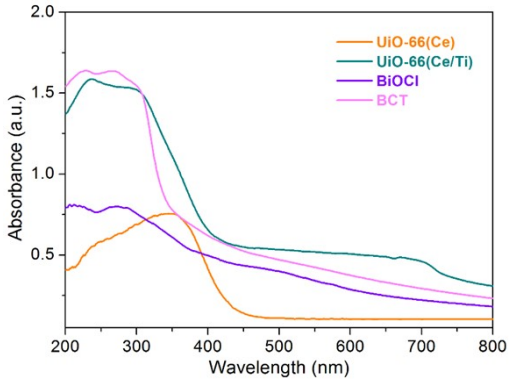

Fig. S3 UV-vis diffuse reflectance spectra of the obtained materials.

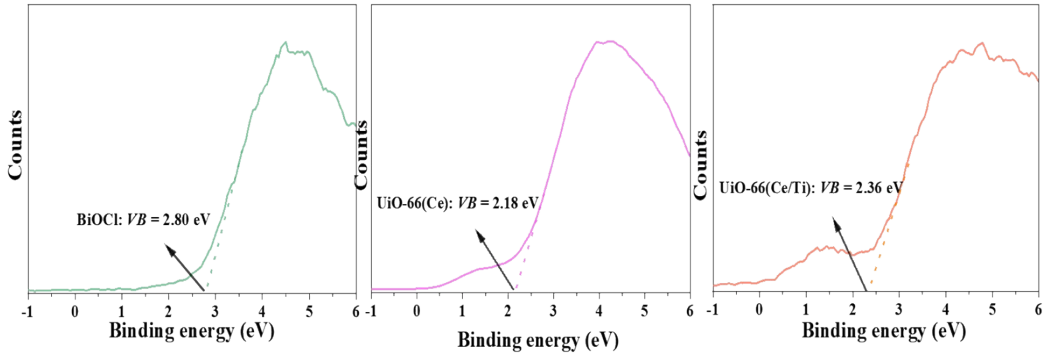

Fig. S4 XPS-VB spectra of the samples.

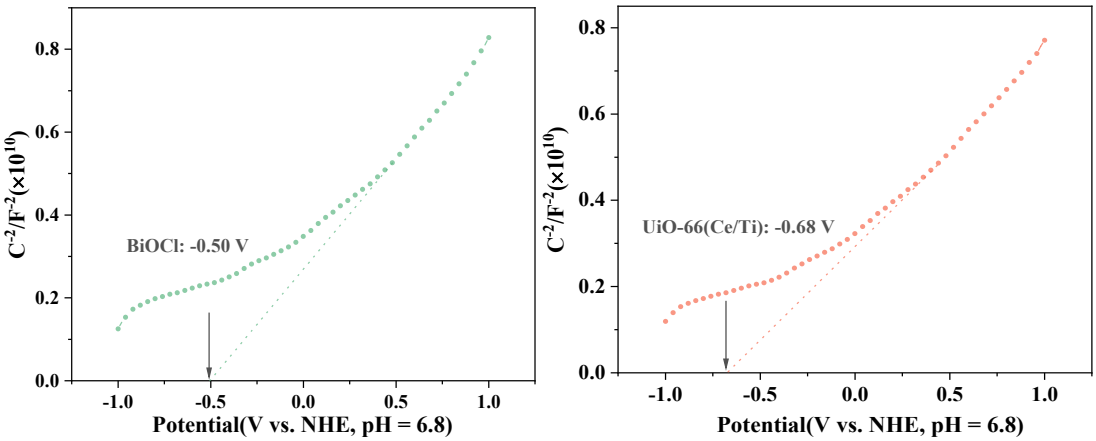

Fig. S5 Mott-Schottky plots of pure BiOCl and UiO-66(Ce/Ti). Experimental conditions: the sample coated on indium-tin-oxide (ITO) glass substrate was applied as the working electrode, Platinum wire and Ag/AgCl electrode were used as the counter electrode and reference electrode, respectively, and 0.1 M Na_2SO_4 solution as the electrolyte.

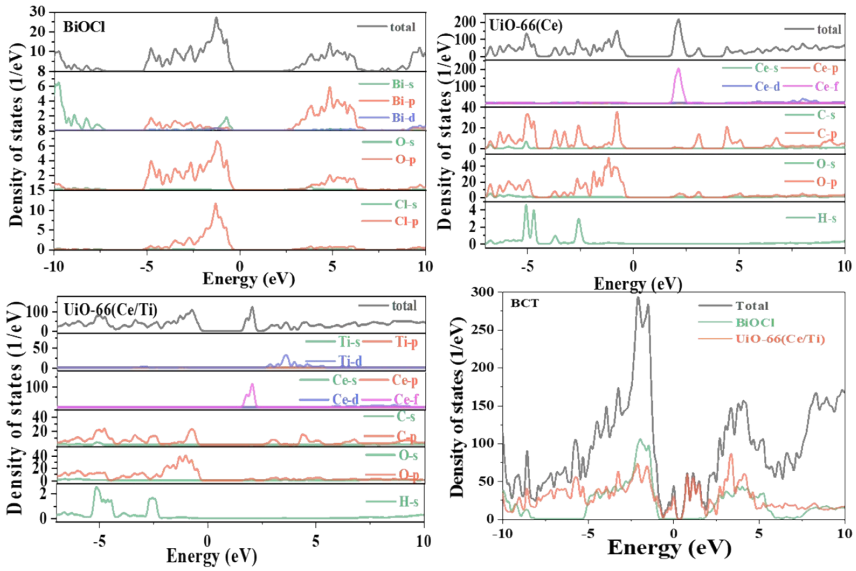

Fig. S6 Total density of states and local density of states of the samples.

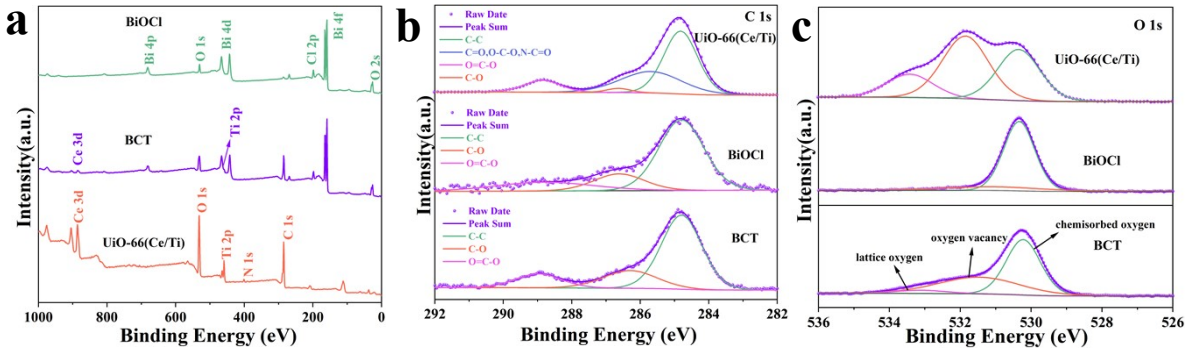

Fig. S7 (a)Full XPS spectra of the samples. High-resolution XPS spectra of (a) C 1s, (b) O 1s in the samples.

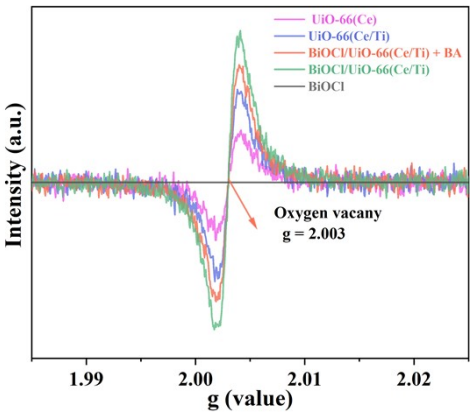

Fig. S8 EPR spectra of samples without UV-Vis irradiation.

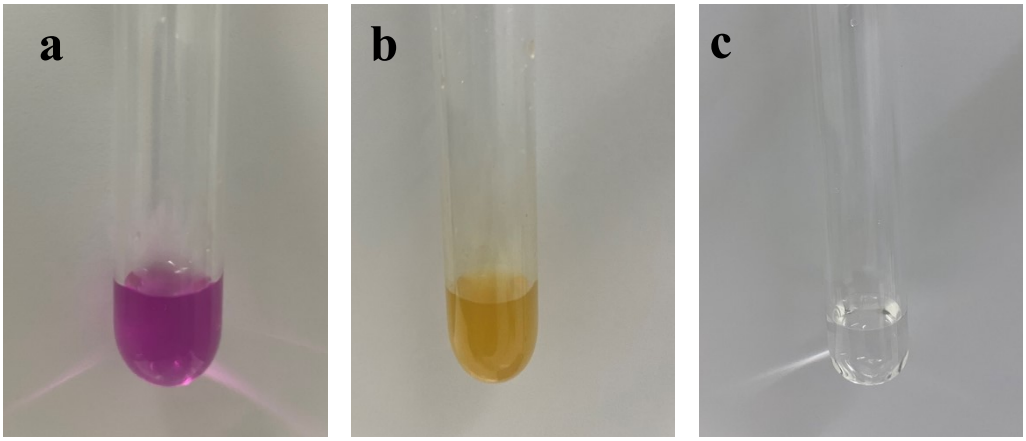

Fig. S9 (a) The aniline solution after adding $KMnO_4$. (b) Add the aniline solution to the $KMnO_4$ with mechanical stirring for 5 min. (c) After filtering the catalyst and light-catalyzed reaction for 30 min, add $KMnO_4$ to the aniline solution. Reaction conditions: KMnO4（1μmol）, benzylamine (0.2 mmol), catalysts (20 mg), H_2O (3 mL), O_2 atmosphere, visible light (λ＞400 nm).

Table S1. Comparison of the photocatalytic activity of BiOCl/UiO-66(Ce/Ti) (BCT) composite with different heterogeneous catalysts for the selective oxidation of benzylamine.

Entry	Catalysts	Conditions	Yield [%]
1	**BCT in this work**	**1 atm O_2, 3 ml H_2O, white LEDs (λ > 400 nm), 6 h**	**98**
2	B-BO-1,3,5[8]	1 atm O_2, 3 ml CH_3CN, 23 W energy saving fluorescent light bulb, 24 h	22
3	TCPP-CMP[9]	1 atm O_2, 10 ml CH_3CN, 100 W white LED, 48 h	76
4	BiOBr-OV[10]	In air, 1 ml CH_3CN, Xe lamp (300 W, > 420 nm), 12 h	96
5	NH2-MIL-125(Ti)[11]	In air, 2 ml CH_3CN, Xe lamp (300 W, > 420 nm), 12 h	73
6	Tx-CMP[12]	1 atm O_2, 5 ml ACN, Natural sunlight, 4 h	78
7	Au-Pt/Cu_7S_4-Cu_9S_8[13]	1 atm O_2, 4 ml DMF, 300 W xenon lamp, 1.5 h	99
8	ZnTEPP-PBI[14]	1 atm O_2, 24 ml MeCN, white LED (90 mW/cm^2), 4 h	99
9	WS_2[15]	50°C, 1 atm O_2, NMP/ACN (10 ml, 3:7), 60 W white LED lamp, 30 h	93
10	Cu_2O/CQD[16]	1 atm O_2, 10 ml CAN, 20 W white LED light, 8 h	95
11	ATA-BiOCl[17]	1 atm O_2, 5 ml ACN, 15 W fluorescent lamp, 24 h	95

12	Au@DUT-67(Zr)[18]	0.1 MPa O_2, 1 mL DMF, visible light ($\lambda \geq 400$ nm), 6h	68

References

1. G. Kresse and D. Joubert, From ultrasoft pseudopotentials to the projector augmented-wave method, *Physical Review B*, 1999, **59**, 1758-1775.
2. G. Kresse and J. Furthmüller, Efficiency of ab-initio total energy calculations for metals and semiconductors using a plane-wave basis set, *Computational Materials Science*, 1996, **6**, 15-50.
3. P. E. Blöchl, Projector augmented-wave method, *Physical Review B*, 1994, **50**, 17953-17979.
4. J. P. Perdew, K. Burke and M. Ernzerhof, Generalized Gradient Approximation Made Simple, *Physical Review Letters*, 1996, **77**, 3865-3868.
5. A. Majid, M. Azmat, U. A. Rana, S. U.-D. Khan and E. Alzahrani, A computational study of magnetic exchange interactions of 3d and 4f electrons in Ti-Ce co-doped AlN, *Materials Chemistry and Physics*, 2016, **179**, 316-321.
6. V. Wang, N. Xu, J.-C. Liu, G. Tang and W.-T. Geng, VASPKIT: A user-friendly interface facilitating high-throughput computing and analysis using VASP code, *Computer Physics Communications*, 2021, **267**, 108033.
7. K. Momma and F. Izumi, VESTA: a three-dimensional visualization system for electronic and structural analysis, *Journal of Applied Crystallography*, 2008, **41**, 653-658.
8. Z. J. Wang, S. Ghasimi, K. Landfester and K. A. I. Zhang, Molecular Structural Design of Conjugated Microporous Poly(Benzooxadiazole) Networks for Enhanced Photocatalytic Activity with Visible Light, *Advanced Materials*, 2015, **27**, 6265-6270.
9. J. Jiang, Z. Liang, X. Xiong, X. Zhou and H. Ji, A Carbazolyl Porphyrin-Based Conjugated Microporous Polymer for Metal-Free Photocatalytic Aerobic Oxidation Reactions, *ChemCatChem*, 2020, **12**, 3523-3529.
10. H. Wang, D. Yong, S. Chen, S. Jiang, X. Zhang, W. Shao, Q. Zhang, W. Yan, B. Pan and Y. Xie, Oxygen-Vacancy-Mediated Exciton Dissociation in BiOBr for Boosting Charge-Carrier-Involved Molecular Oxygen Activation, *Journal of the American Chemical Society*, 2018, **140**, 1760-1766.
11. D. Sun, L. Ye and Z. Li, Visible-light-assisted aerobic photocatalytic oxidation of amines to imines over NH_2-MIL-125(Ti), *Applied Catalysis B: Environmental*, 2015, **164**, 428-432.
12. V. R. Battula, H. Singh, S. Kumar, I. Bala, S. K. Pal and K. Kailasam, Natural Sunlight Driven Oxidative Homocoupling of Amines by a Truxene-Based Conjugated Microporous Polymer, *ACS Catalysis*, 2018, **8**, 6751-6759.
13. H. Gao, Y. Chen, H. Li, F. Zhang and G. Tian, Hierarchical Cu_7S_4-Cu_9S_8 heterostructure hollow cubes for photothermal aerobic oxidation of amines,

Chemical Engineering Journal, 2019, **363**, 247-258.
14. X.-X. Guo, J. Jiang, Q. Han, X.-H. Liu, X.-T. Zhou and H.-B. Ji, Zinc porphyrin-based electron donor–acceptor-conjugated microporous polymer for the efficient photocatalytic oxidative coupling of amines under visible light, *Applied Catalysis A: General*, 2020, **590**, 117352.
15. F. Raza, J. H. Park, H.-R. Lee, H.-I. Kim, S.-J. Jeon and J.-H. Kim, Visible-Light-Driven Oxidative Coupling Reactions of Amines by Photoactive WS_2 Nanosheets, *ACS Catalysis*, 2016, **6**, 2754-2759.
16. A. Kumar, A. Hamdi, Y. Coffinier, A. Addad, P. Roussel, R. Boukherroub and S. L. Jain, Visible light assisted oxidative coupling of benzylamines using heterostructured nanocomposite photocatalyst, *Journal of Photochemistry and Photobiology A: Chemistry*, 2018, **356**, 457-463.
17. A. Han, J. Sun, H. Zhang, G.-K. Chuah and S. Jaenicke, Visible Light Induced Selective Aerobic Formation of N-benzylidene Benzylamine over 2-aminoterephthalic Acid Sensitized {110}-Facetted BiOCl Nanosheets, *ChemCatChem*, 2019, **11**, 6425-6430.
18. C. Liu, Y. Liu, Y. Shi, Z. Wang, W. Guo, J. Bi and L. Wu, Au nanoparticles-anchored defective metal–organic frameworks for photocatalytic transformation of amines to imines under visible light, *Journal of Colloid and Interface Science*, 2023, **631**, 154-163.